Yang *et al. Chem Synth* 2024;4:68
DOI: 10.20517/cs.2024.105

Chemical Synthesis

Research Highlight

Open Access

Ultrafast S-scheme interfacial electron transport enhances CO_2 photoreduction

Jindi Yang, Chuanbiao Bie*

UQ Dow Centre for Sustainable Engineering Innovation, School of Chemical Engineering, The University of Queensland, St Lucia 4067, QLD, Australia.

***Correspondence to:** Dr. Chuanbiao Bie, UQ Dow Centre for Sustainable Engineering Innovation, School of Chemical Engineering, The University of Queensland, Andrew N. Liveris Building, 46 Staff House Road, St Lucia 4067, QLD, Australia. E-mail: biechuanbiao@cug.edu.cn

How to cite this article: Yang J, Bie C. Ultrafast S-scheme interfacial electron transport enhances CO_2 photoreduction. *Chem Synth* 2024;4:68. https://dx.doi.org/10.20517/cs.2024.105

Received: 24 Aug 2024 **First Decision:** 26 Sep 2024 **Revised:** 27 Sep 2024 **Accepted:** 16 Oct 2024 **Published:** 6 Nov 2024

Academic Editor: Aicheng Chen **Copy Editor:** Ting-Ting Hu **Production Editor:** Ting-Ting Hu

Keywords: S-scheme heterojunctions, interfacial electron transfer, photocatalysis, CO_2 reduction

The increasing gap between CO_2 emissions from human activities and the carbon capture and sequestration capabilities of natural ecosystems has intensified the focus on achieving global net-zero carbon emissions[1-3]. Photocatalytic CO_2 reduction, which transforms CO_2 into high-value-added fuels or chemicals, presents a promising strategy for reaching carbon neutrality[4-6]. However, challenges associated with photocatalysts, such as limitations in light absorption, rapid recombination of photogenerated carriers, and kinetic barriers, significantly hinder CO_2 photoconversion efficiency[7]. As a result, the development of efficient photocatalysts to improve CO_2 reduction efficiency has become a key research priority in the field of photocatalysis[8,9].

Among various photocatalyst design strategies, S-scheme heterojunctions composed of reduction and oxidation semiconductors have gained significant attention[10,11]. Compared with single-component photocatalysts and type-II heterojunctions, S-scheme heterojunctions not only facilitate efficient separation of photogenerated carriers but also enhance redox capacity, providing a distinct advantage for CO_2 photoreduction[12-14]. However, low-quality interfaces in these heterojunctions often impede efficient interfacial electron transport, thereby limiting overall photocatalytic efficiency.

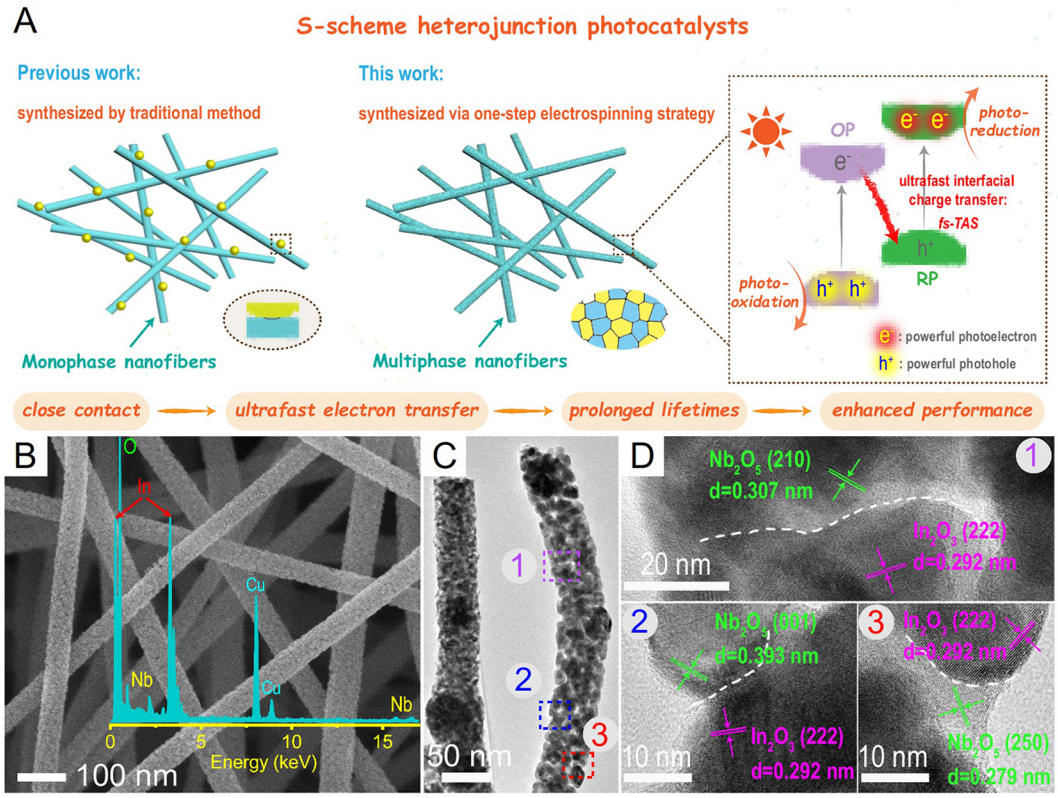

Figure 1. (A) Schematic illustration and design concept of the study; (B) Field emission scanning electron microscopy image and energy-dispersive X-ray spectrum; (C) TEM image; and (D) high-resolution TEM images of the In_2O_3/Nb_2O_5 heterojunctions (IN10). This figure is quoted with permission from Deng *et al.*[15]. OP: Oxidation photocatalysts; RP: reduction photocatalysts; fs-TAS: femtosecond transient absorption spectroscopy.

To address this issue, Deng et al. recently developed an S-scheme In_2O_3/Nb_2O_5 heterojunction photocatalyst, denoted as IN*x*[15]. In this designation, "I" stands for In_2O_3, "N" represents Nb_2O_5, and "*x*" indicates the weight percentage of Nb_2O_5 relative to In_2O_3. This catalyst was prepared using a one-step high-temperature calcination process after electrospinning the precursor into fibers [Figure 1A]. Unlike conventional two- or multi-step synthesis strategies, this "one-pot" approach allowed for the simultaneous synthesis of In_2O_3 and Nb_2O_5, ensuring optimal contact between the two components. Transmission electron microscopy (TEM) images revealed that the close contact between In_2O_3 and Nb_2O_5 created an extensive two-phase interface, significantly enhancing carrier transport efficiency [Figure 1B-D]. This design strategy created a high-quality carrier transport channel, facilitating efficient interfacial charge transfer.

Femtosecond transient absorption spectroscopy indicated that the ground-state bleach (GSB) signal of In_2O_3 is attributed to photogenerated electrons[Figure 2], as confirmed by using $AgNO_3$ as an electron scavenger. In pristine In_2O_3, photogenerated electrons undergo interband diffusion and shallow trap state capture [Figure 2A and E]. However, in the S-scheme In_2O_3/Nb_2O_5 heterojunction, a new process is observed: the transfer of photogenerated electrons from the conduction band of In_2O_3 to the valence band of Nb_2O_5 [Figure 2B and F]. Under an argon atmosphere, increasing the Nb_2O_5 content in the heterojunction reduces interband diffusion and shallow trap state capture due to competition with the S-scheme interfacial electron transfer [Figure 2C]. In a CO_2 environment, the consumption of electrons by CO_2 further intensifies this competition, resulting in S-scheme electron transfer occurring in less than 10 ps [Figure 2D and G]. This rapid transfer suppresses electron recombination and significantly extends electron lifetime.

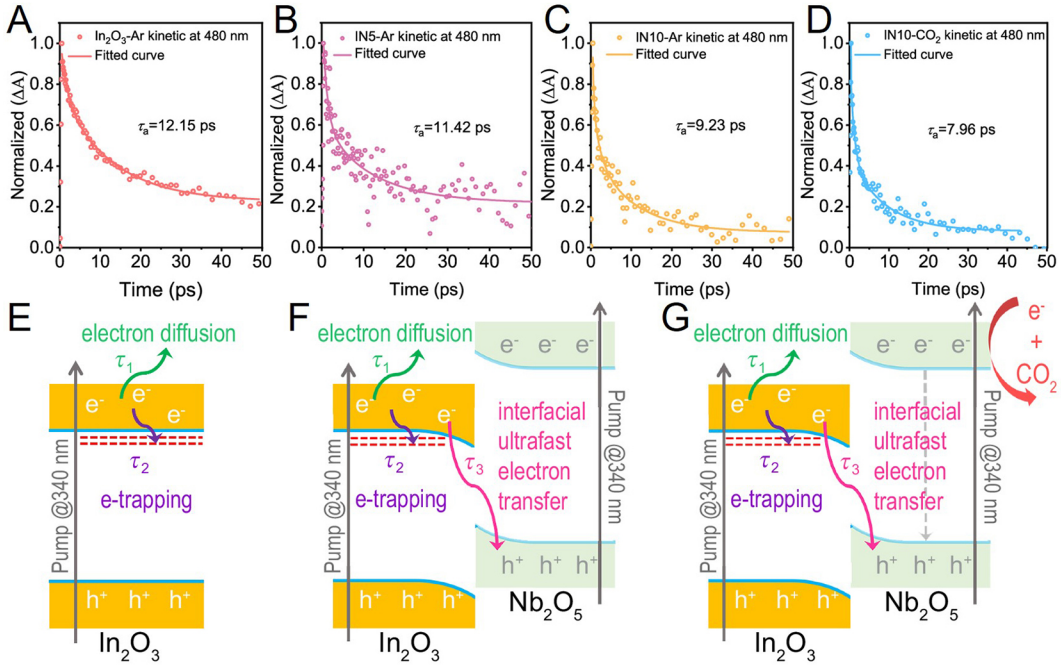

Figure 2. Charge carrier dynamic decay for (A) pure In_2O_3 in Ar; (B) IN5 in Ar; (C) IN10 in Ar; and (D) IN10 in CO_2; schematic illustrations of the decay pathways of photogenerated electrons in (E) pure In_2O_3; (F) In_2O_3/Nb_2O_5 heterojunctions in Ar; and (G) In_2O_3 /Nb_2O_5 heterojunctions in CO_2. This figure is quoted with permission from Deng *et al.*[15].

In contrast, the GSB signal of Nb_2O_5 was attributed to photogenerated holes[Figure 3], as verified by using lactic acid as a hole scavenger. In Nb_2O_5, photogenerated holes participate in recombination with both intrinsic photogenerated electrons and electrons transferred from In_2O_3 [Figure 3A and E]. Under an argon atmosphere, the half-life of photogenerated holes in Nb_2O_5 within the In_2O_3/Nb_2O_5 heterojunction is shorter than that in pristine Nb_2O_5 due to rapid hole consumption by ultrafast interfacial electron transfer [Figure 3B and F]. When Nb_2O_5 content is excessive, In_2O_3 photogenerated electrons cannot fully consume the Nb_2O_5 photogenerated holes, resulting in an extended hole lifetime [Figure 3C]. In a CO_2 atmosphere, although CO_2 reacts with photogenerated electrons, reducing hole consumption, it also accelerates the transfer of electrons from In_2O_3 to the valence band of Nb_2O_5 and increases hole recombination. Thus, the lifetime of photogenerated holes in the heterojunction does not significantly differ between CO_2 and argon atmospheres [Figure 3D and G].

Photocatalytic CO_2 reduction experiments demonstrated that the primary product across all samples was CO, exhibiting nearly 100% selectivity [Figure 4A]. Pure In_2O_3 and Nb_2O_5 displayed poor photocatalytic performance due to the rapid recombination of photogenerated carriers inherent to single-phase photocatalysts. However, the formation of S-scheme heterojunctions significantly enhanced CO yield, achieving a maximum CO_2-to-CO conversion activity of 0.21 mmol·$g_{active\ sites}^{-1}$·h^{-1} for IN10. Furthermore, the significance of close interfacial contact between the two phases in promoting ultrafast interfacial electron transfer within the S-scheme heterojunction was validated by comparing the CO_2 photoreduction activities of IN10, In_2O_3/Nb_2O_5 nanohybrids synthesized via the conventional impregnation-calcination method, and physical mixtures of In_2O_3 and Nb_2O_5 [Figure 4B]. Additionally, isotopically labeled experiments revealed three mass spectral signals at m/z = 13, 16, and 29, corresponding to the fragments of ^{13}C, O, and ^{13}CO, respectively [Figure 4C]. These findings confirm the absence of interference from exogenous carbon sources in the origin of the products.

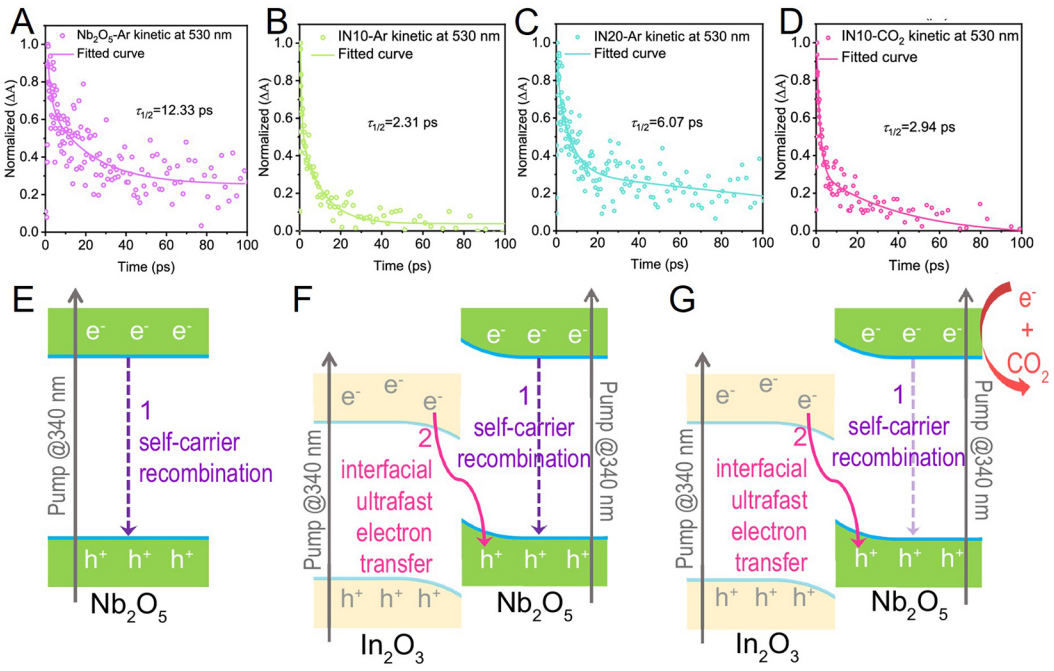

Figure 3. Charge carrier dynamic decay for (A) pure Nb_2O_5 in Ar; (B) IN20 in Ar; (C) IN10 in Ar; and (D) IN10 in CO_2; schematic illustrations of the decay pathways of photogenerated holes in (E) pure Nb_2O_5; (F) In_2O_3/Nb_2O_5 heterojunctions in Ar; and (G) In_2O_3/Nb_2O_5 heterojunctions in CO_2. This figure is quoted with permission from Deng *et al.*[15].

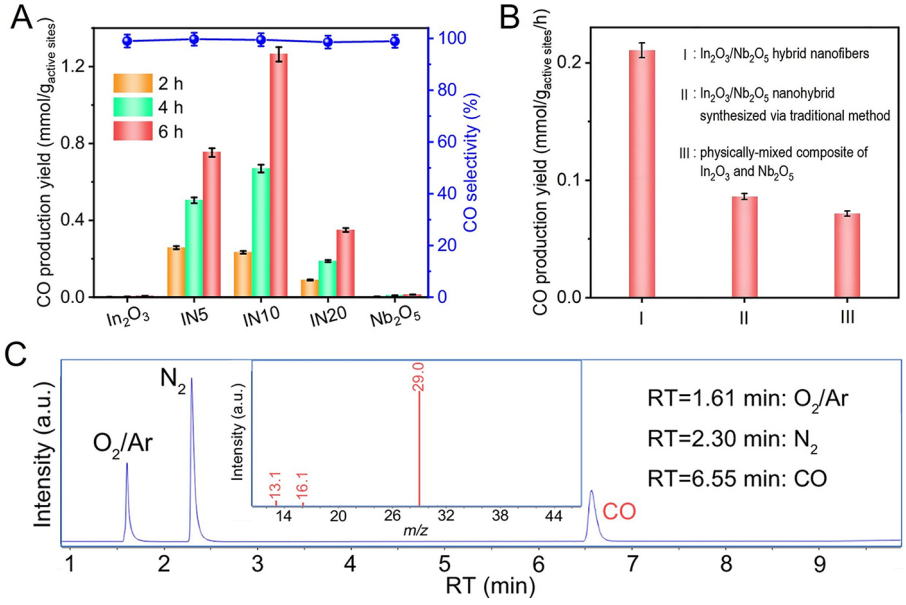

Figure 4. (A) Production yields and CO selectivity over In_2O_3, INx, and Nb_2O_5; (B) Comparison of CO_2 photoreduction performance among various In_2O_3/Nb_2O_5 composites; (C) Total ion chromatography and corresponding mass spectra of products from the photocatalytic reduction of $^{13}CO_2$ over IN10. RT denotes retention time. This figure is quoted with permission from Deng *et al.*[15].

In summary, this work has significantly enhanced CO_2 photoreduction efficiency by developing an S-scheme In_2O_3/Nb_2O_5 heterojunction photocatalyst with high-quality interfacial transport channels. It underscores the critical role of high-quality heterojunction interfaces in achieving ultrafast carrier transport

and provides valuable insights for the design of future heterojunction photocatalysts.

DECLARATIONS

Authors' contributions

Wrote the draft manuscript: Yang J
Revised and rewrote the manuscript: Bie C

Availability of data and materials

Not applicable.

Financial support and sponsorship

This work was supported by the National Natural Science Foundation of China (22202187), the National Postdoctoral Program for Innovative Talents (BX2021275), the Project funded by China Postdoctoral Science Foundation (2022M712957), and the Postdoctoral Funding Program of Hubei Province. Chuanbiao Bie acknowledges financial support from the China Scholarship Council.

Conflicts of interest

All authors declared that there are no conflicts of interest.

Ethical approval and consent to participate

Not applicable.

Consent for publication

Not applicable.

REFERENCES

1. Tang J, Weiss E, Shao Z. Advances in cutting-edge electrode engineering toward CO_2 electrolysis at high current density and selectivity: a mini-review. *Carbon Neutralization* 2022;1:140-58. DOI
2. Bie C, Meng Z, He B, Cheng B, Liu G, Zhu B. Exploring photogenerated charge carrier transfer in semiconductor/metal junctions using Kelvin probe force microscopy. *J Mater Sci Technol* 2024;173:11-9. DOI
3. Yin Y, Kang X, Han B. Two-dimensional materials: synthesis and applications in the electro-reduction of carbon dioxide. *Chem Synth* 2022;2:19. DOI
4. Xie F, Bie C, Sun J, Zhang Z, Zhu B. A DFT study on Pt single atom loaded COF for efficient photocatalytic CO_2 reduction. *J Mater Sci Technol* 2024;170:87-94. DOI
5. Wu D, Tian C, Zhou J, et al. Morphology and structure of lead-free CuSb-based double perovskites for photocatalytic CO_2 reduction. *Carbon Neutralization* 2022;1:298-305. DOI
6. Bie C, Zhang L, Yu J. Graphene oxide-based photocatalysts for CO_2 reduction. In: Yu J, Zhang L, Kuang P, editors. Graphene oxide-metal oxide and other graphene oxide-based composites in photocatalysis and electrocatalysis. Elsevier; 2022. pp. 93-134. DOI
7. Hiragond CB, Powar NS, Kim H, In S. Unlocking solar energy: photocatalysts design for tuning the CO_2 conversion into high-value (C_{2+}) solar fuels. *EnergyChem* 2024;6:100130. DOI
8. Vuong H, Nguyen D, Phuong LP, Minh PPD, Ho BN, Nguyen HA. Nitrogen-rich graphitic carbon nitride (g-C_3N_5): emerging low-bandgap materials for photocatalysis. *Carbon Neutralization* 2023;2:425-57. DOI
9. Li Y, Zhang D, Qiao W, et al. Nanostructured heterogeneous photocatalyst materials for green synthesis of valuable chemicals. *Chem Synth* 2022;2:9. DOI
10. Bie C, Yu J. Application of S -scheme heterojunction photocatalyst. In: Wang X, Anpo M, Fu X, editors. UV-visible photocatalysis for clean energy production and pollution remediation. Wiley; 2023. pp. 41-58. DOI
11. Meng K, Zhang J, Cheng B, et al. Plasmonic near-infrared-response S-scheme ZnO/$CuInS_2$ photocatalyst for H_2O_2 production coupled with glycerin oxidation. *Adv Mater* 2024;36:e2406460. DOI PubMed
12. Li F, Yue X, Liao Y, Qiao L, Lv K, Xiang Q. Understanding the unique S-scheme charge migration in triazine/heptazine crystalline

carbon nitride homojunction. *Nat Commun* 2023;14:3901. DOI PubMed PMC

13. Zhang L, Zhang J, Yu H, Yu J. Emerging S-scheme photocatalyst. *Adv Mater* 2022;34:e2107668. DOI PubMed
14. Yu W, Bie C. Unveiling S-scheme charge transfer mechanism. *Acta Phys Chim Sin* 2024;40:2307022. DOI
15. Deng X, Zhang J, Qi K, Liang G, Xu F, Yu J. Ultrafast electron transfer at the In_2O_3/Nb_2O_5 S-scheme interface for CO_2 photoreduction. *Nat Commun* 2024;15:4807. DOI PubMed PMC